Submitted to ApJ

# New Planets around three G Dwarfs [1]

Simon J. O'Toole[2], R. Paul Butler[3], C. G. Tinney[2], Hugh R. A. Jones[4], Geoffrey W. Marcy[5,7], Brad Carter[6], Chris McCarthy[7], Jeremy Bailey[8], Alan J. Penny[9], Kevin Apps[10], Debra Fischer[7,5]

## ABSTRACT

Doppler velocity measurements from the Anglo-Australian Planet Search reveal planetary mass companions to HD 23127, HD 159868, and a possible second planetary companion to HD 154857. These stars are all G dwarfs. The companions are all in eccentric orbits with periods ranging from 1.2 to $> 9.3\,\mathrm{yr}$, minimum ($M \sin i$) masses ranging from 1.5 to $> 4.5\,\mathrm{M_J}$, and semimajor axes between 1 and $> 4.5\,\mathrm{AU}$. The orbital parameters are updated for the inner planet to HD 154857, while continued monitoring of the outer companion is required to confirm its planet status.

*Subject headings:* planetary systems – stars: individual (HD 23127, HD 159868, HD 154857)

---

[1]Based on observations obtained at the Anglo–Australian Telescope, Siding Spring, Australia.

[2]Anglo–Australian Observatory, P.O. Box 296, Epping, NSW 1710, Australia

[3]Department of Terrestrial Magnetism, Carnegie Institution of Washington, 5241 Broad Branch Road NW, Washington DC, USA 20015-1305

[4]Centre for Astrophysics Research, University of Hertfordshire, Hatfield, AL 10 9AB, UK

[5]Department of Astronomy, University of California, Berkeley, CA USA 94720

[6]Faculty of Sciences, University of Southern Queensland, Toowoomba, Queensland 4350, Australia

[7]Department of Physics and Astronomy, San Francisco State University, San Francisco, CA, USA 94132

[8]Australian Centre for Astrobiology, Macquarie University, Sydney, NSW 2109, Australia

[9]University of St Andrews, School of Physics and Astronomy, North Haugh, St Andrews, UK

[10]Physics and Astronomy, University of Sussex, Falmer, Brighton BN1 9QJ, UK

## 1. Introduction

As extrasolar planetary research enters its second decade, the field continues to be driven by precision Doppler surveys. Roughly 95% of all known planets come from such surveys, including all of the ∼180 extrasolar planets[1] orbiting stars within 100 pc (Butler et al. 2006).

The most promising new methods for the detection and study of nearby exoplanets are the next generation techniques of interferometric astrometry and direct imaging. However, these have proven harder to develop and implement than expected a decade ago. Over the same period Doppler programs have steadily improved their precision from 10 to $1\,\mathrm{m\,s^{-1}}$. At this level, precision Doppler surveys will remain the dominant detection technique for exoplanets orbiting nearby stars for the foreseeable future.

The Anglo-Australian Planet Search (AAPS) began observing 200 stars in January 1998. In 2002 the program expanded from 20 to 32 nights per year. In response two changes were made: 60 new stars were added, and observations with signal-to-noise ratios of at least 200 became the goal for all survey stars. The AAT target list has been published in Jones et al. (2002).

A total of 26 planets have emerged from the AAT program. The full set of AAT Doppler velocity measurements for these stars are included in the "Catalog of Nearby Exoplanets" (Butler et al. 2006). These AAT velocities have already yielded a new 300 day planet orbiting HD 160691 (Gozdiewski et al. 2006), which has been subsequently confirmed with HARPS data (Pepe et al. 2006). In this paper three new AAT planets are announced.

## 2. Observations

Precision Doppler velocity measurements are made at the 3.9-m Anglo-Australian Telescope (AAT) with the UCLES echelle spectrograph (Diego et al. 1990). A 1″ slit yields $\lambda/\Delta\lambda \sim 50000$ spectra that span the wavelength range from 4820–8550 Å. An iodine absorption cell (Marcy & Butler 1992) provides wavelength calibration from 5000 to 6100 Å. The spectral point-spread function is derived from the detailed shapes of the embedded iodine lines (Valenti et al. 1995). The precision Doppler analysis is carried out with an updated version of the technique outlined by Butler et al. (1996). The long-term underlying systematic precision of the AAPS as demonstrated by stable stars is $3\,\mathrm{m\,s^{-1}}$(see e.g. Figures 1-4 of Butler et al. 2001, Figure 1 of McCarthy et al. 2004, Figure 1 of Tinney et al. 2005). Only

[1]cf. list of exoplanets orbiting nearby stars at www.exoplanets.org at 1 October 2006

the Doppler program at Keck has demonstrated a similar level of precision on time scales of many years (see Figures in Vogt et al. 2000, Butler et al. 2004, Marcy et al. 2005, Vogt et al. 2005, Rivera et al. 2005, and Butler et al. 2006).

## 3. Three New Planets

The physical parameters for the planet-bearing stars reported in this paper are listed in Table 1. All three of these stars are classified as G dwarfs in the Michigan Catalog (Houk & Cowley 1975, 1978, 1982). The stellar distances are from HIPPARCOS (Perryman et al. 1997). The estimates of stellar activity ($R'_{HK}$) are from Jenkins et al. (2006). The metallicity and $v \sin i$ measurements are from Valenti & Fischer (2005) based on spectral synthesis matched to high-resolution ($\lambda/\Delta\lambda \sim 66,000$) iodine-free "template" spectra, taken with a 0.75″ slit. The estimates of stellar mass and age are from the analysis of Takeda et al. (2006). The estimated intrinsic stellar Doppler jitter is from our latest upgrade to the calibration of Wright (2005).

The absolute magnitudes of these stars range from $M_v = 3.8$ to $M_v = 3.0$, suggesting they have all begun to evolve off the main sequence, consistent with their estimated stellar ages (5.6 to 8 Gyr), and with the measured level of chromospheric activity and $v \sin i$ velocities.

### 3.1. HD 159868

This star has been observed 28 times since being added to the AAPS program when it was expanded in 2002. These data are listed in Table 2 and shown in Figure 2. The root-mean-square (RMS) of these velocities about the mean is $29\,\mathrm{m\,s^{-1}}$, exceeding that expected from the photon-counting internal measurement precision and stellar jitter. (The median value of the internal measurement uncertainties is $1.4\,\mathrm{m\,s^{-1}}$, while the estimated intrinsic stellar jitter for HD 159868 of $\sim 2\,\mathrm{m\,s^{-1}}$.)

We are in the process of developing a modified detection algorithm based on an improved version of the Lomb-Scargle (LS) periodogram (Lomb 1976; Scargle 1982). The standard LS technique estimates power in a time-series of data by fitting sinusoids at fixed periods to generate a periodogram. However, planets do not necessarily (indeed it would seem only infrequently) lie in the circular orbits which result in sinusoidal Doppler variations. Ideally one would fit Keplerians, however this requires generating a periodogram which is a function of both period *and* eccentricity.

We have therefore generated what we call "two dimensional Keplerian Lomb-Scargle"

(2DKLS) periodograms, which are formed by fitting Keplerians at a grid of periods and eccentricities, and then calculating power using Equation 7 of Cumming (2004). The period at maximum power in the period-eccentricity plane, is then used as an initial estimate for a non-linear least-squares Keplerian fit, this time varying all the Keplerian free parameters until the minimum reduced $\chi^2$ ($\chi^2_\nu$) is determined. The uncertainties quoted in this paper are derived from the diagonal terms in the covariance matrix, and only represent a true estimation of the uncertainty on the fitted parameters in the absence of degeneracy between those parameters. As a general rule, Keplerian fits usually have some degeneracy between semi-amplitude ($K$) and eccentricity ($e$), resulting in the uncertainty estimates on those terms being a lower limit.

Figure 1 demonstrates the 2DKLS with the Doppler data for HD 159868. The upper panel shows the 2DKLS power spectrum in greyscale, while the lower panels show the power spectrum resulting at fixed eccentricities of $e = 0$ (left) and 0.69 (right). The former therefore corresponds to a "standard" Lomb-Scargle periodogram (ie. fitting sinusoids), and the latter is a cut at the eccentricity corresponding to peak power in the 2DKLS. The lower left panel of Figure 1 (i.e. for $e = 0$) indicates maximum power at $P = 1343\,\mathrm{d}$, while that at the 2DKLS peak power in the lower right panel is $P = 986\,\mathrm{d}$. The Keplerian resulting from a non-linear least-squares solution is shown as a dashed line in Figure 2, and has semi-amplitude $K$=$43.3\,\mathrm{m\,s^{-1}}$, giving a minimum planetary mass $M \sin i$=$1.7\,\mathrm{M_J}$, and a semimajor axis $a$=2.0 AU.

Figure 1 demonstrates some of the features of the 2DKLS method. The contrast in these power spectra is considerably higher at the eccentricity corresponding to peak 2DKLS power than at $e = 0$. Moreover, the period at which the power peak occurs is significantly different. Using the standard LS as an initial estimate to the non-linear Keplerian fitting process does eventually generate a best-fit period near 2DKLS peak power period. However, using the intial estimate derived from the 2DKLS is clearly preferable.

Throughout the remainder of this paper, when we present power spectra, these will actually be cuts through the 2DKLS at the eccentricity corresponding to the peak power in the 2DKLS (which is noted).

The $\chi^2_\nu$ of the best-fit Keplerian is 15.22, and the RMS is $8.5\,\mathrm{m\,s^{-1}}$, which is still significantly larger than expected based on internal meaurement uncertainties and jitter. Though a component of this excess RMS could be due to asteroseismological "noise" (as discussed by Tinney et al. 2005), it is unlikely to be the sole cause. So, while the Keplerian false alarm probability (FAP – calculated as described in Marcy et al. 2005) for this fit is quite low ($< 10^{-3}$), the large residuals have motivated a search for additional companions.

Allowing for a long term linear trend makes no significant improvement to the RMS or $\chi^2_\nu$. Planets with shorter periods can be fitted simultaneously with the planet reported here, and solutions obtained that significantly improve the RMS and $\chi^2_\nu$. For example a 180 d, $M \sin i$=0.5 $M_J$, $e$=0.05 planet reduces the joint RMS to 4.5 m s$^{-1}$and $\chi^2_\nu$ to 4.4. However, the parameters of such a solution are poorly constrained by the available sampling, so no definitive statement can be made about the orbital properties of a possible second planet around HD 159868.

### 3.2. HD 23127

HD 23127 was added to the AAPS program in late 1998 together with 19 other targets, following suggestions that metal-rich stars preferentially host exoplanets (see e.g. Laughlin 2000 and references therein). Tinney et al. (2003) describes this metal-rich subsample and its selection. A total of 34 observations (listed in Table 4) have been taken over 7.7 years beginning 1998 October. The RMS of these velocities about the mean is 25 m s$^{-1}$, again exceeding that expected based on photon-counting internal measurement precision and stellar jitter. (The median value of the internal measurement uncertainties is 4.4 m s$^{-1}$; estimated stellar jitter is ∼2.0 m s$^{-1}$.) Examination of Table 4 shows how our precision (as determined by the internal uncertainty estimates listed in the table) has significantly improved in recent years as exposure times have been increased from ∼5 to ∼20 minutes to meet our higher S/N goal.

The power spectrum for HD 23127 is shown in Figure 4 at an eccentricity of 0.44, corresponding to peak power in the 2DKLS. The peak at ∼1214 d (3.33 yr) is clear. The best-fit Keplerian is shown as the dashed line in Figure 3. The RMS of the residuals (11.1 m s$^{-1}$) and $\chi^2_\nu$ of the fit (5.11) are both high. These are due to the lower precision and larger scatter of the earliest measurements and partially because of the star's faintness. (If the residuals are divided in two, we find an RMS of 13.2 m s$^{-1}$ before 2003 and 4.8 m s$^{-1}$ after.) The minimum mass ($M \sin i$) of the planet is 1.5 $M_J$, and the semi-major axis is 2.4 AU.

### 3.3. HD 154857

HD 154857 was added to our target list when the AAPS was expanded in 2002. As discussed in McCarthy et al. (2004) this star has evolved about 2 magnitudes above the main sequence. Based on 18 observations made between 2002 April and 2004 February, McCarthy et al. announced a first planet around this star, with a period of ∼400 d, and an

additional linear trend suggesting a second longer period companion.

A total of 28 AAT observations of HD 154857, spanning 4.5 years, are listed in Table 5 and plotted in Figure 5. The velocity RMS of the raw data set is $35\,\mathrm{m\,s^{-1}}$. The median internal measurement uncertainty is $1.7\,\mathrm{m\,s^{-1}}$, and the estimated stellar jitter is $2.6\,\mathrm{m\,s^{-1}}$. The dashed line shows the best-fit single Keplerian with a linear trend, with an orbital period of 1.1 yr and an eccentricity of 0.52, in agreement with McCarthy et al. The RMS of the velocities to the Keplerian plus linear trend is $7.77\,\mathrm{m\,s^{-1}}$ and the $\chi^2_\nu$ is 7.51.

Over the past two years the combination of a single Keplerian plus linear trend has provided a systematically poorer match to the data. We have therefore been motivated to search for a two Keplerian solution. Figure 6 shows best-fit double Keplerian, which was found by starting with the single-Keplerian parameters for the known planet. The updated orbital parameters for the inner planet (Table 3) from this fit are basically consistent with those given by McCarthy et al. (2004), and with four full orbits observed, these parameters are now well constrained. The fit parameters for the outer planet are $P$=7.94 yr, $K$=466.5 $\mathrm{m\,s^{-1}}$, and $e$=0.87. The minimum mass is $M \sin i$=18.4 $\mathrm{M_J}$ and $a$=4.3 AU. The RMS to the two Keplerian fit is $3.68\,\mathrm{m\,s^{-1}}$, with a $\chi^2_\nu$ of 1.73. The parameters of the (outer) long-period companion of HD 154857 are not well constrained; fitting very long periods leads to poorly determined eccentricities and $M \sin i$ values in the brown dwarf regime or larger. More observations are needed to constrain the parameters of this object, while robust lower limits are provided in Table 3.

## 4. Discussion

Thirty planets have now emerged from the 260 target stars of the AAPS, suggesting that ∼10% of late F, G, and K field dwarfs have planets that can be detected with Doppler precisions of $3\,\mathrm{m\,s^{-1}}$ and a time baseline of 8 years (a similar detection rate to that of the original 106 stars on the Lick Observatory survey which has yielded 13 planets to date; Fischer et al. 2003). These surveys are now beginning to explore planets in orbits beyond 4 AU, though they remain insensitive to terrestrial mass planets beyond 0.1 AU and neptune-mass planets beyond 1 AU. However, with planets being found orbiting more than 10% of nearby sun-like stars, it seems that planetary systems are common.

For the current high precision Doppler surveys, the one detectable signpost of a Solar System analog is a giant planet in a circular orbit ($e < 0.1$) beyond 4 AU, with no giant planets interior to 4 AU. Previously five giant planets orbiting beyond 4 AU have been found. Of these, only 55 Cnc has an outer planet in such a circular orbit, however, it also has two

giant planets orbiting at 0.11 and 0.23 AU. The outer planet orbiting HD 217107 (Vogt et al. 2005; Wittenmyer et al. 2006) has an eccentricity of 0.55 and an interior giant planet in a 7 d orbit. The planets orbiting HD 72659 (Butler et al. 2006), HD 154345 and HD 24040 (Wright et al. 2007) have eccentricities of 0.27, 0.52, and 0.20 respectively.

In this paper an additional object, possibly a giant planet (HD 154857c) are presented, orbiting at (or beyond) 4 AU and with quite high eccentricity. Thus five of the six planets orbiting beyond 4 AU, are in eccentric orbits, and the sixth has giant planets in inner orbits. The distribution of eccentricities for planets beyond 4 AU is similar to that for planets between 0.2 and 4 AU, and there is no indication of a trend for increased circularity in planets orbiting at large radii. This suggests that while gas-giant planets themselves are common (orbiting $\gtrsim 10\%$ of sun-like stars), Solar System analogs may not be as common. Over the next decade the number of planets detected beyond 4 AU will grow enabling us to determine accurately whether Solar System analogs are rare or not. However, to understand completely the frequency of these detections, we will need to more thoroughly simulate the selection functions implicit in our observing strategies. The AAPS program, along with other Doppler searches, has been underway for more than 8 years. To date no detailed simulation and analysis of these selection functions has yet been undertaken by AAPS or any other planet search. What is needed is to not only determine what can be detected using our current observational techniques and sampling, but what should have been detected but has not been, if we are to constrain the underlying frequency distributions of planets and planetary system parameters. An effort in this direction is now well underway for the AAPS.

We gratefully acknowledge the superb technical support at the Anglo-Australian Telescope which has been critical to the success of this project – in particular we acknowledge R. Paterson, D. Stafford, S. Lee, J. Pogson and J. Stevenson. We acknowledge support by PPARC grant PPC/C000552/1 (SJOT), NSF grant AST-9988087 and travel support from the Carnegie Institution of Washington (RPB), NASA grant NAG5-8299 and NSF grant AST95-20443 (GWM). We thank the Australian and UK Telescope assignment committees (ATAC & PATT) for generous allocations of telescope time. This research has made use of NASA's Astrophysics Data System, and the SIMBAD database, operated at CDS, Strasbourg, France.

## REFERENCES

Butler, R. P., Marcy, G. W., Williams, E., McCarthy, C., Dosanjh, P., & Vogt, S. S. 1996, PASP , 108, 500

Butler, R. P., Tinney, C. G., Marcy, G. W., Jones, H. R. A., Penny, A. J. & Apps, K. 2001, ApJ , 555, 410.

Butler, R. P., Vogt, S. S., Marcy, G. W., Fischer, D. A., Wright, J. J., Henry, G. W., Laughlin, G. & Lissauer, J. J. 2004, ApJ , 617, 580.

Butler, R. P., Wright, J. T., Marcy, G. W., Fischer, D. A., Vogt, S. S., Tinney, C. G., Jones, H. R. A., Carter, B. D., Johnson, J. A., McCarthy, C. & Penny, A. J. 2006, ApJ , 646, 505.

Cumming, A. 2004, MNRAS, 354, 1165.

Diego, F., Charalambous, A., Fish, A. C., & Walker, D. D. 1990, Proc. Soc. Photo-Opt. Instr. Eng., 1235, 562

Fischer, D. A., Marcy, G. W., Butler, R. P., Vogt, S. S., Henry, G. W., Pourbaix, D., Walp, B., Misch, A. A. & Wright, J. T. 2003, ApJ, 586, 1394.

Gozdziewski, Maciejewski, A. J. & Migaszewski, C. 2006, ApJ, , accepted.

Houk, N. & Cowley, A. P. 1975, *Michigan Catalog of Two Dimensional Spectral Types for the HD Stars, Vol. 1*, (Ann Arbor, University of Michigan).

Houk, N. & Cowley, A. P. 1978, *Michigan Catalog of Two Dimensional Spectral Types for the HD Stars, Vol. 2*, (Ann Arbor, University of Michigan).

Houk, N. & Cowley, A. P. 1982, *Michigan Catalog of Two Dimensional Spectral Types for the HD Stars, Vol. 3*, (Ann Arbor, University of Michigan).

Jenkins, J. S., Jones, H. R. A., Tinney, C. G., Butler, R. P., McCarthy, C., Marcy, G. W., Pinfield, D. J., Carter, B. D., & Penny, A. J. 2006, MNRAS , 372, 163.

Jones, H. R. A., Butler, R. P., Marcy, G. W., Tinney, C. G., Penny, A. J., McCarthy, C., & Carter, B. D. 2002, MNRAS , 337, 1170.

Laughlin, G. 2000, ApJ , 545, 1064.

Lomb, N. R. 1976, Ap&SS, 39, 447.

McCarthy, Chris, Butler, R. Paul, Tinney, C. G., Jones, Hugh R. A., Marcy, Geoffrey W., Carter, Brad, Penny, Alan J. & Fischer, Debra A. 2004, ApJ, 617, 575.

Marcy, G. W. & Butler, R. P. 1992, PASP , 104, 270.

Marcy, G. W., Butler, R. P., Vogt, S. S., Fischer, D. A., Henry, G. W., Laughlin, G., Wright, J. T. & Johnson, J. A. 2005, ApJ , 619, 570.

Perryman, M. A. C., et al. 1997, A&A , 323, L49. The Hipparcos Catalog

Pepe, F, Correia, A., Mayor, M., Tamuz, O., Benz, W., Bertaux, J.L., Bouchy, F., Couetdic, J., Laskar, J., Lovis, C., Naef, D., Queloz, D., Santos, N., Sivan, J.P., Sosnowska, D. & Udry, S. 2006 A&A, accepted.

Rivera, E. J., Lissauer, J. J., Butler, R. P., Marcy, G. W., Vogt, S. S., Fischer, D. A., Brown, T. M., Laughlin, G. & Henry, G. W. 2005, ApJ , 634, 625.

Scargle, J. D. 1982, ApJ , 263, 865.

Takeda, G., Ford, E. B., Sills, A., Rasio, F. A., Fischer, D. A., & Valenti, J. A. 2006, ApJS, submitted.

Tinney, C. G., Butler, R. P., Marcy, G. W., Jones, H. R. A., Penny, A. J., McCarthy, C., Carter, B. D., & Bond, J. 2003, ApJ, 587, 423.

Tinney, C. G., Butler, R. Paul, Marcy, Geoffrey W., Jones, Hugh R. A., Penny, Alan J., McCarthy, Chris, Carter, Brad D. & Fischer, Debra A. 2005, ApJ, 623, 1171.

Valenti, J., Butler, R. P., & Marcy, G. W. 1995, PASP , 107, 966

Valenti, J. & Fischer, D. A. 2005, ApJS, 159, 141.

Vogt, S. S., Marcy, G. W., Butler, R. P., & Apps,K. 2000, ApJ, 536, 902

Vogt, S. S., Butler, R. P., Marcy, G. W., Fischer, D. A., Henry, G. W., Laughlin, G., Wright, J. T. & Johnson, J. J. 2005, ApJ, 632, 638.

Wittenmyer, R. A., Endl, M., & Cochran, W. D. 2006. ApJ , in press.

Wright, J. T. 2005, PASP , 117, 657.

Wright, J. T., Marcy, G. W., Fischer, D. A., Butler, R. P., Vogt, S. S., Tinney, C. G., Jones, H. R. A., Carter, B. D., Johnson, J. A. McCarthy, C. & Apps, K. 2007, ApJ, in press, to appear in 20 Feb 2007 issue 656.

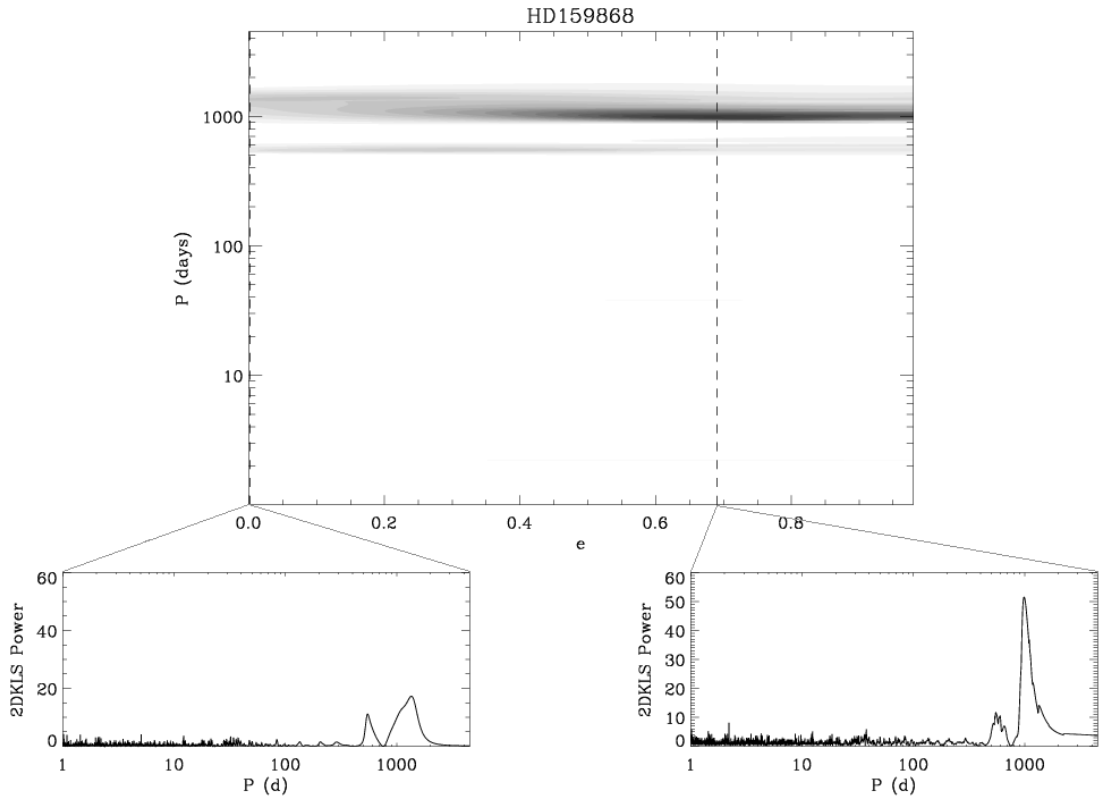


Fig. 1.— 2D Keplerian Lomb-Scargle (2DKLS) periodogram for HD 159868. The upper panel shows the 2DKLS, the lower left panel shows the power spectrum generated at $e = 0$, and the lower right panel shows the power spectrum at $e = 0.69$ corresponding to the peak power in the 2DKLS. The power spectrum at $e = 0.69$ clearly shows higher contrast, and a different period to that at $e = 0$ (which corresponds to a "standard" Lomb-Scargle periodigram).

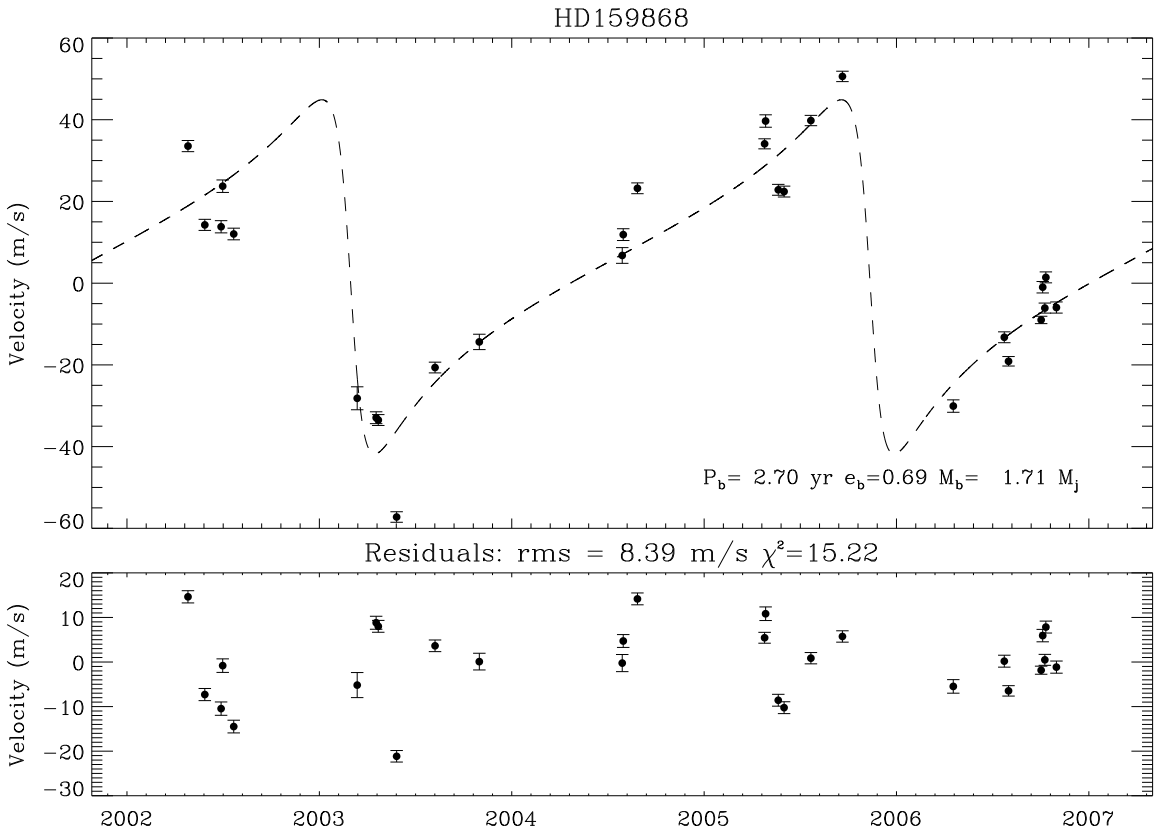


Fig. 2.— Keplerian fit to HD 159868. The RMS to a single Keplerian model is significantly higher than the internal measurement error, which combined with the high $\chi^2_\nu$ is suggestive of a second companion.

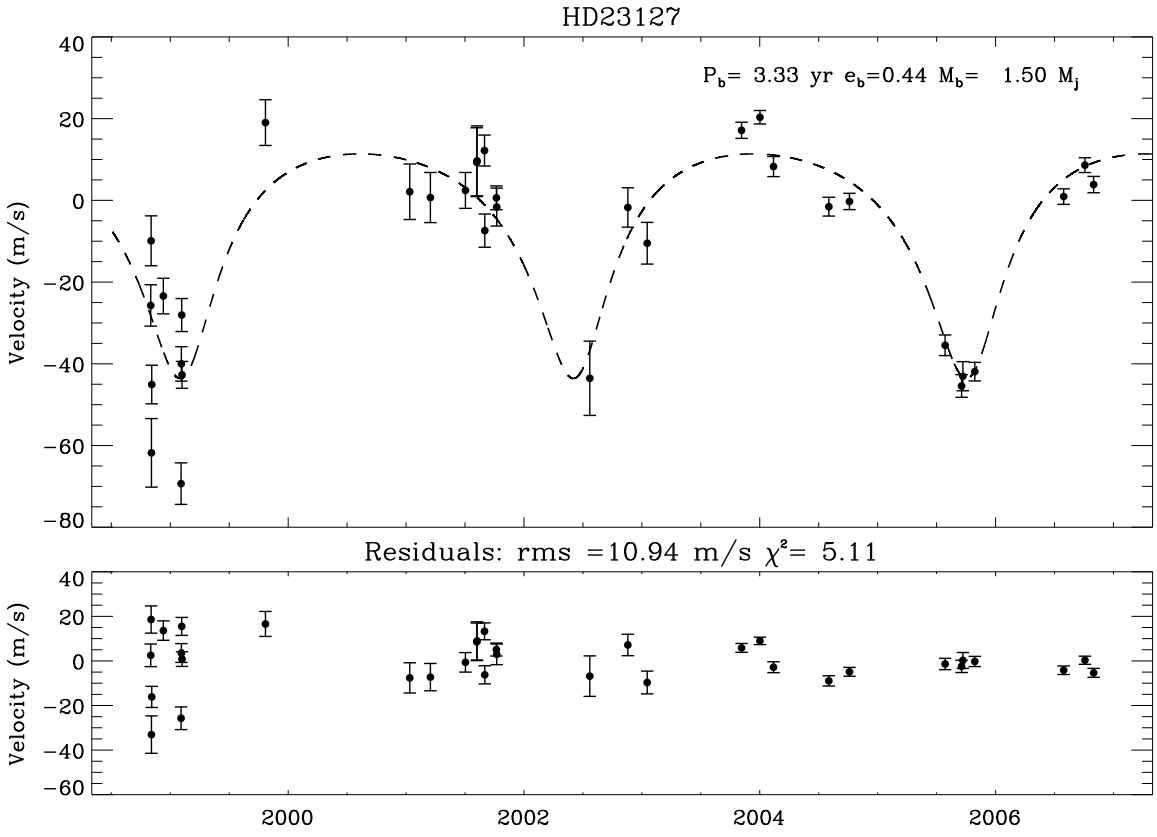


Fig. 3.— Doppler velocities for HD 23127, with the best–fit Keplerian (dashed line). Most of the scatter in the Keplerian fit is due to first epoch observations. The observations taken over the first few years have signal–to–noise of ∼50, compared to later observations with S/N ∼100.

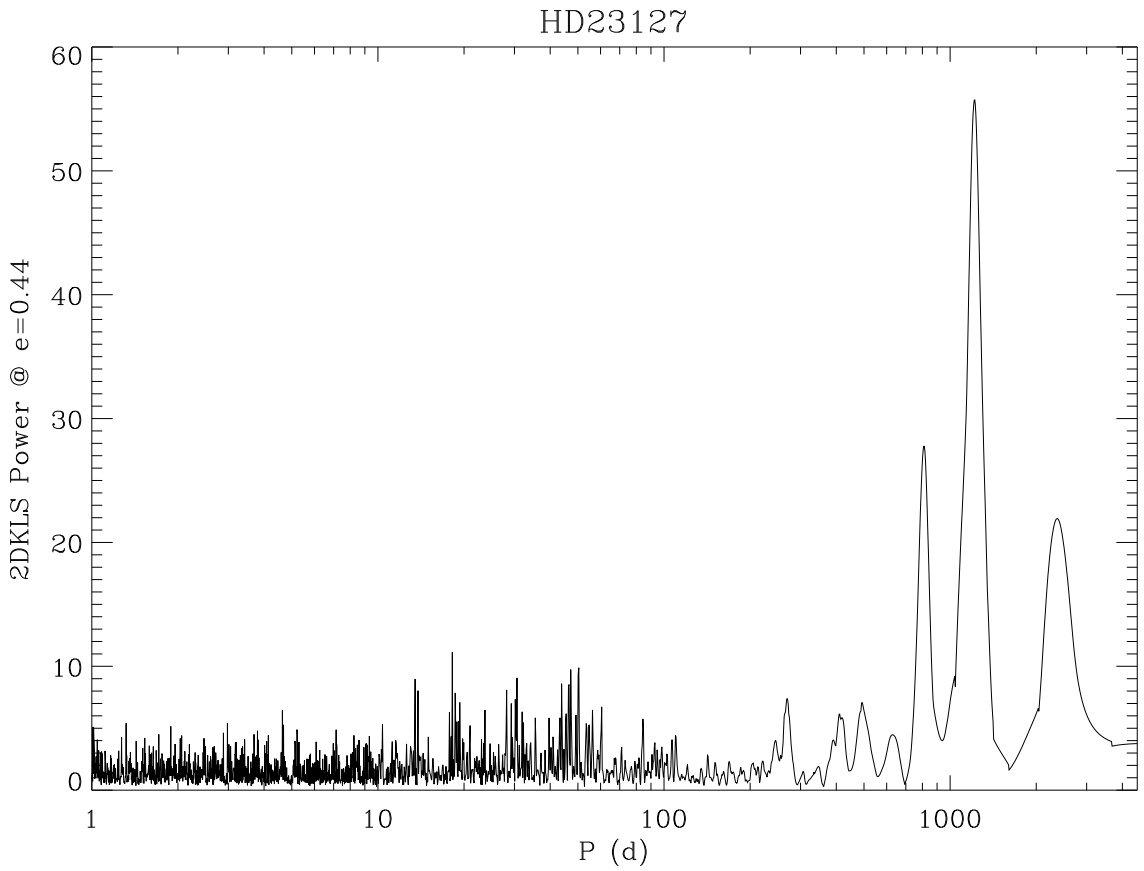


Fig. 4.— 2D Keplerian Lomb-Scargle periodogram for HD 23127 at $e$=0.44 showing significant power at 1214 d or 3.33 yr.

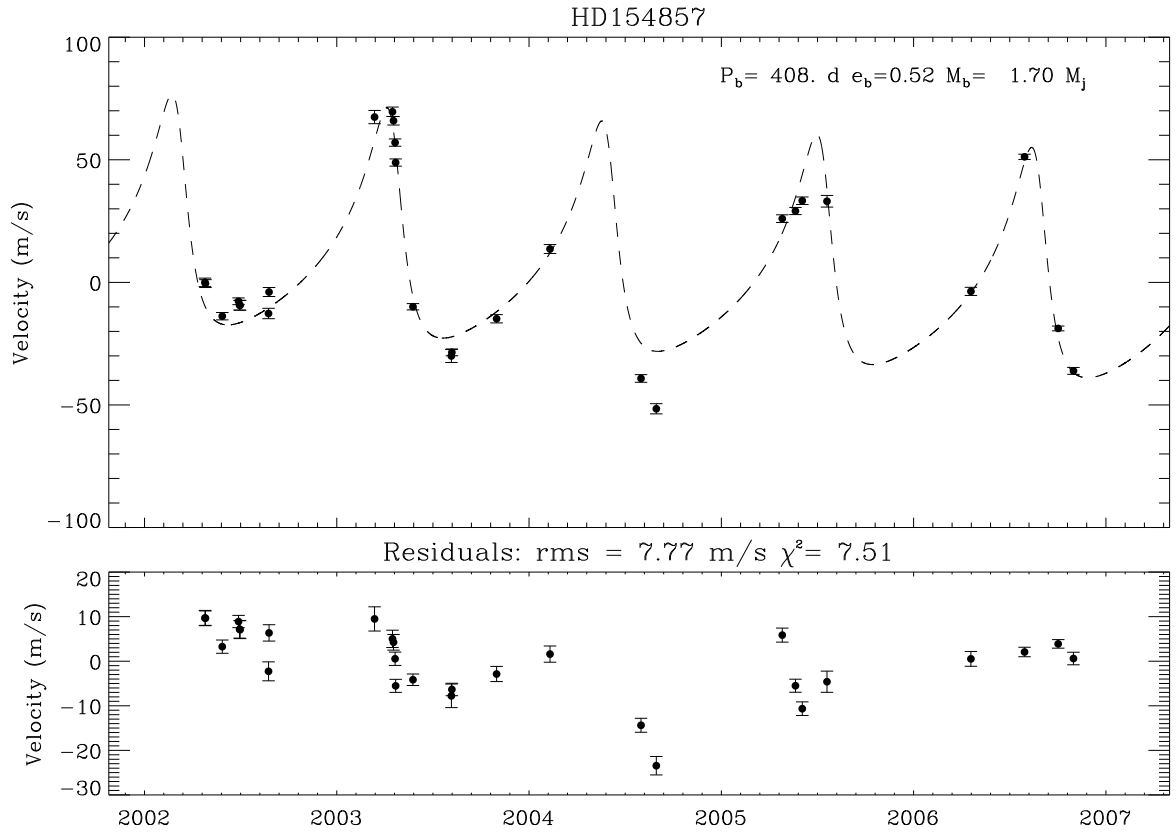


Fig. 5.— A single Keplerian fit including a linear trend for HD 154857. There is still a systematic variation present in the residuals and their RMS is still much higher than the internal measurement uncertainties.

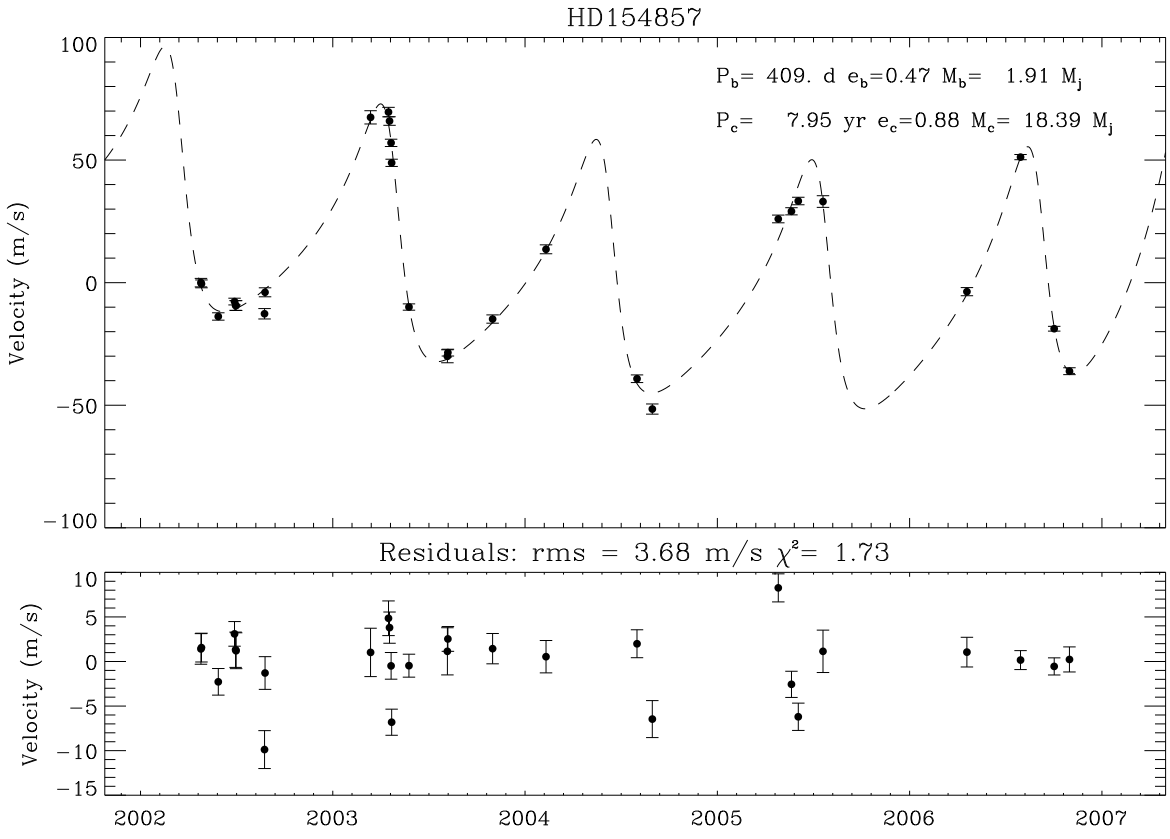


Fig. 6.— A double Keplerian fit for HD 154857. Fitting the second planet significantly improves the $\chi^2_\nu$, although its period and eccentricity are not well constrained.

Table 1. Stellar Properties of Planet-bearing Stars[a]

| Star (HD) | Star (HIP) | Spec. Type | B-V | V | $M_V$ | Mass ($M_\odot$) | $R'_{HK}$ | $v \sin i$ ($km\,s^{-1}$) | Age (Gyr) | Jitter ($m\,s^{-1}$) | [Fe/H] | |
|---|---|---|---|---|---|---|---|---|---|---|---|---|
| 23127 | 17054 | G2V | 0.69 | 8.58 | 3.82 | 1.13 | −5.00 | 3.3 | 7.1[b] | 2.0 | +0.34 | 8 |
| 159868 | 86375 | G5V | 0.72 | 7.24 | 3.07 | 1.09 | −4.96 | 2.1 | 8.1 | 2.0 | +0.00 | 5 |
| 154857 | 84069 | G5V | 0.65 | 7.24 | 3.63 | 1.17 | −5.00 | 1.4 | 5.6 | 2.6 | −0.22 | 6 |

[a]See Section 3 for details on the references and derivations of the physical parameters in this Table. Ty
uncertainties on these parameters are $M_V \pm 0.2$, mass $\pm 0.10$, $R'_{HK} \pm 0.04$, $v \sin i \pm 0.5$, Age $\pm 1.0$, Jitter $\pm 0.5$
[Fe/H] $\pm 0.05$.

[b]ower limit for HD 23127 is 4.2 Gyr.

Table 2. Velocities for HD 159868

| JD (-2450000) | RV ($m\,s^{-1}$) |
|---|---|
| 2390.2278 | 28.7 ± 1.3 |
| 2422.1471 | 10.5 ± 1.4 |
| 2453.0426 | 10.2 ± 1.5 |
| 2456.0712 | 19.6 ± 1.6 |
| 2477.0206 | 7.9 ± 1.5 |
| 2711.2689 | -32.3 ± 2.7 |
| 2747.2526 | -37.8 ± 1.4 |
| 2751.2604 | -38.1 ± 1.3 |
| 2786.1000 | -60.9 ± 1.3 |
| 2858.9541 | -24.5 ± 1.3 |
| 2942.9349 | -18.6 ± 1.9 |
| 3214.0987 | 2.9 ± 1.9 |
| 3216.0451 | 7.9 ± 1.4 |
| 3242.9683 | 19.2 ± 1.4 |
| 3484.2386 | 29.7 ± 1.2 |
| 3486.1651 | 35.3 ± 1.5 |
| 3510.1739 | 19.7 ± 1.3 |
| 3521.1956 | 18.4 ± 1.3 |
| 3572.0699 | 35.7 ± 1.2 |
| 3631.8981 | 46.5 ± 1.3 |
| 3842.2411 | -34.0 ± 1.5 |
| 3939.0094 | -17.4 ± 1.3 |
| 3947.0564 | -23.5 ± 1.1 |
| 4008.9180 | -9.0 ± 0.9 |
| 4011.9102 | -1.0 ± 1.4 |
| 4015.9496 | -6.1 ± 1.2 |
| 4017.8979 | 1.4 ± 1.3 |
| 4037.8961 | -6.0 ± 1.4 |

Table 3. Orbital Parameters[a]

| Star (HD) | Period (days) | $K$ ($\mathrm{m\,s^{-1}}$) | $e$ | $\omega$ (°) | $T_0$ (JD-2450000) | $M \sin i$ ($\mathrm{M_J}$) | $a$ (AU) | $\mathrm{N}_{obs}$ | RMS ($\mathrm{m\,s^{-1}}$) |
|---|---|---|---|---|---|---|---|---|---|
| 159868 | 986(9) | 43.3(2) | 0.69(0.02) | 97(3) | 700(9) | 1.7(0.3) | 2.0(0.3) | 28 | 4.08 |
| 23127 | 1214(9) | 27.5(1) | 0.44(0.07) | 190(6) | 229(19) | 1.5(0.2) | 2.4(0.3) | 34 | 12.6 |
| 154857b | 409.0(1) | 50.4(1) | 0.47(0.02) | 59(4) | 346(5) | 1.8(0.4) | 1.2(0.2) | 28 | 5.03 |
| 154857c[b] | 1900: | 23: | 0.25: | | | | | 28 | 5.03 |

[a]These values are the best-fit results from the 2DKLS algorithm. $\omega$ and $T_0$ are the angle of periastron and periastron passage time, respectively. Uncertainties are indicated in parentheses, estimated as described in the text.

[b]Numbers quoted with colons represent a robust lower limit; higher values produce a negligible difference in $\chi^2_\nu$.

Table 4. Velocities for HD 23127

| JD (-2450000) | RV ($m\,s^{-1}$) |
|---|---|
| 1118.0928 | -14.4 ± 5.1 |
| 1119.1769 | 1.5 ± 6.1 |
| 1120.2630 | -50.4 ± 8.4 |
| 1121.1204 | -33.7 ± 4.7 |
| 1157.1101 | -12.0 ± 4.4 |
| 1211.9789 | -58.0 ± 5.1 |
| 1212.9583 | -28.7 ± 4.2 |
| 1213.9930 | -16.7 ± 4.0 |
| 1214.9443 | -31.3 ± 3.3 |
| 1473.2455 | 30.4 ± 5.6 |
| 1920.0076 | 13.5 ± 6.8 |
| 1983.8817 | 12.1 ± 6.1 |
| 2092.3152 | 13.8 ± 4.4 |
| 2127.2891 | 20.7 ± 8.4 |
| 2128.3130 | 21.0 ± 8.6 |
| 2151.3089 | 23.6 ± 3.8 |
| 2152.1997 | 4.0 ± 4.1 |
| 2188.1530 | 12.4 ± 2.9 |
| 2189.1692 | 12.3 ± 4.7 |
| 2477.3358 | -32.3 ± 8.9 |
| 2595.0910 | 7.8 ± 4.8 |
| 2655.0337 | 0.3 ± 4.9 |
| 2947.1369 | 29.7 ± 2.0 |
| 3004.0254 | 31.7 ± 1.7 |
| 3045.9962 | 20.0 ± 2.4 |
| 3217.3038 | 10.1 ± 2.3 |
| 3281.2209 | 11.0 ± 2.0 |
| 3577.3179 | -24.2 ± 2.5 |
| 3628.2861 | -34.6 ± 2.7 |
| 3632.2557 | -31.3 ± 3.5 |

Table 4—Continued

| JD (-2450000) | RV ($m\,s^{-1}$) |
|---|---|
| 3669.2013 | -30.1 ± 2.3 |
| 3944.3322 | 12.0 ± 1.8 |
| 4010.1981 | 8.6 ± 1.8 |
| 4037.1442 | 3.9 ± 2.0 |

Table 6. Velocities for HD 154857

| JD (-2450000) | RV ($m\,s^{-1}$) |
|---|---|
| 2389.2358 | -17.1 ± 1.7 |
| 2390.2122 | -17.4 ± 1.6 |
| 2422.1371 | -30.2 ± 1.5 |
| 2453.0201 | -24.3 ± 1.4 |
| 2455.0253 | -25.8 ± 2.0 |
| 2455.9766 | -26.0 ± 2.0 |
| 2509.9485 | -29.5 ± 2.1 |
| 2510.9162 | -20.4 ± 1.9 |
| 2711.2461 | 50.4 ± 2.8 |
| 2745.2425 | 52.6 ± 1.9 |
| 2747.2118 | 48.8 ± 1.8 |
| 2750.1777 | 40.0 ± 1.5 |
| 2751.2295 | 31.8 ± 1.4 |
| 2784.1265 | -26.9 ± 1.3 |
| 2857.0297 | -47.0 ± 2.6 |
| 2857.9859 | -45.6 ± 1.4 |
| 2942.9121 | -31.9 ± 1.7 |
| 3044.2691 | -3.1 ± 1.8 |
| 3217.0121 | -56.0 ± 1.6 |
| 3246.0381 | -68.0 ± 2.0 |
| 3485.1521 | 8.8 ± 1.6 |
| 3510.1595 | 12.3 ± 1.5 |
| 3523.1016 | 16.1 ± 1.6 |
| 3570.0292 | 16.0 ± 2.4 |
| 3843.2397 | -20.8 ± 1.6 |
| 3945.0325 | 34.6 ± 1.1 |
| 4008.8962 | -18.8 ± 1.0 |
| 4037.8808 | -36.1 ± 1.4 |